

# Barotropic Instability of the African Easterly Jet and its potential for development

Marangelly Fuentes <sup>1</sup>

Howard University Program in Atmospheric Sciences (HUPAS)  
Howard University, Washington, DC

Mentor: Oreste Reale

Laboratory for Atmospheres,  
NASA Goddard Space Flight Center, Greenbelt, Maryland  
and  
Goddard Earth Sciences and Technology Center,  
University of Maryland, Baltimore County, Baltimore, Maryland

---

<sup>1</sup>Corresponding author's address: Marangelly Fuentes, 12904 Falling Water Circle Apt. 202 Germantown, MD 20874. E-mail: marangelly.fuentes@gmail.com

# 1 Abstract

This work was developed during a summer internship at the Laboratory for atmospheres at the NASA Goddard Space Flight Center, and made possible by the GEST Center Graduate Student Summer Program (GSSP). The preliminary part of the activity involved training on the analysis of large model-generated atmospheric gridded data sets, including the usage of meteorology-oriented graphics tools. The focus of this work is the analysis of the high-resolution NASA finite volume General Circulation Model (fvGCM) representation of barotropic instability in the African Easterly Jet, and its contribution to cyclogenetic processes. The model is based on a finite volume dynamical core with terrain-following Lagrangian control, volume dynamical discretization, and performs efficiently on massive parallel architectures. In the past GCMs did not fully resolve tropical cyclones and therefore tropical cyclogenesis was generally very difficult to reproduce. Ten simulations of Atlantic Tropical systems in 2004, between August and September, are analyzed. The choice is made because of the simultaneous appearance of a developing system (Hurricane Frances) and a non-developing one. The model creates a barotropically unstable column throughout the entire troposphere only at the center of the developing system. These findings are suggestive that barotropic instability plays some role in the early tropical development, as represented in the fvGCM.

## 2 Introduction

### 2.1 Background

The preliminary part of the activity developed at the Laboratory for Atmospheres at the NASA Goddard Space Flight Center during this internship involved an extensive training on: 1) general atmospheric dynamics; 2) tropical cyclones; 3) analysis of atmospheric gridded data sets; 4) development of diagnostic tools with the aid of the Graphical Analysis and Display System (GrADS). This training was a prerequisite to start the actual scientific investigation which was focused on the representation of barotropic instability in the NASA finite volume General Circulation Model (fvGCM) as one of the contributing mechanisms to Atlantic tropical cyclogenesis.

Four kinds of atmospheric instabilities are known: conditional instability of the first kind (hereafter CIFK), conditional instability of the second kind (hereafter CISK), baroclinic instability and barotropic instability. CIFK is the state of a layer of unsaturated air when its lapse rate of temperature is less than the dry-adiabatic lapse rate [Holton, 2004] but greater than the moist-adiabatic lapse rate. Under such conditions a parcel of air at the environmental temperature is unstable to upward vertical displacements if it is saturated, unstable to downward displacements if it is saturated and contains cloud water, but stable to all small vertical displacements if it is unsaturated. Release of CIFK on a large horizontal scale affects also the dynamical stability of the atmosphere. This can happen to such an extent that

the vertical shears which are otherwise stable with respect to dry adiabatic vertical motion, become unstable with respect to the saturated adiabatic vertical motion.

CIFK can originate another dynamic instability which is called CISK [Ooyama, 1964 and Charney and Eliassen, 1964]. CISK is a process where diabatic heating due to latent heat released by cumulus clouds produces a large-scale(or mesoscale) cyclonic disturbance. This disturbance, through boundary layer pumping, drives the low-level moisture convergence necessary to maintain an environment favorable for the development of cumulus convection [Holton, 2004]. The atmospheric environment that favors CISK is found over warm, tropical oceans where there is an abundant supply of moisture, the Coriolis force is small, and low-level convergence is strong.

The wave instabilities important for synoptic-scale meteorology are theoretically described in the form of zonally asymmetric perturbations to a zonally symmetric basic flow field. In general the basic flow is a jetstream that has both horizontal and vertical mean-flow shears [Holton, 2004]. Baroclinic instability arises from the combination of vertical shear of the mean flow and rotation. They grow by converting potential energy associated with the mean horizontal temperature gradient that must exist to provide thermal wind balance from the vertical shear in the basic state flow [Holton, 2004]. Midlatitude cyclones grow mainly because of baroclinic instability. Satellite imagery of baroclinic cyclones reveals an asymmetric cloud pattern with no eyelike feature. The thermal structure is asymmetrical, with cold advection

generally to the north and to the west of the surface low, and warm advection to the south and to the east [Reale and Atlas, 2000].

In contrast, barotropic instability is a wave instability that arises from horizontal shear in a jet. Waves grow by extracting kinetic energy from the mean-flow field [Holton, 2004] through horizontal non-divergent motions. This extraction of kinetic energy occurs between the basic flow and the wave perturbations. Kuo (1949) investigated the concept of barotropic instability of a zonal flow. He considered the shear flow on the rotating earth and treated continuous variation of velocity in the direction normal to the velocity direction [Asnani, 2005], along with, variations in latitude with time  $U(y, t)$  and having a non zero meridional velocity shear  $\frac{\partial U}{\partial y}$ , symmetrical with respect to certain latitude [Reale and Atlas, 2000]. Kuo(1949) defined a critical point ( $y = y_k$ ) as the latitude where the absolute vorticity of the zonal flow has a maximum or a minimum applying a linearized theory and a non-vertical shear atmosphere where  $\beta - \frac{\partial^2 U}{\partial y^2} = 0$ . He concluded that a wave can grow at the expenses of the kinetic energy of a zonal current. The verification of Kuo's necessary condition for barotropic instability  $K(y) = \frac{\partial}{\partial y}[f(y) - \frac{\partial U}{\partial y}] = 0$  can be an indicator of where barotropic instability is possible, in response to the shear of the zonal flow.

## 2.2 Tropical Cyclones in GCMs

General Circulation Models (GCMs) have generally not been considered suitable to properly represent TCs because of the inadequate resolution necessary

to fully resolve the cyclone's structure [e.g. Hou et al., 2004]. There are several difficulties in the numerical forecast of TCs, the most important being the scale, which is of the order of hundreds of km. The resolution needed to resolve the fine structure of the TC circulation would be in the order of 10-20 km or higher [e.g. Kurihara, 1990], whereas global models used for operational weather forecasting until one or two years ago operate at a resolution of 50-100km. As a consequence, the vortices represented in GCMs are too weak, their scale is too large, and their fine structure is not properly represented [Atlas et al., 2005b]. The only models which can resolve the structure of TC were regional models, which have limited area domains and are forced by the boundary conditions produced by GCMs. Various techniques to improve the initialization and, therefore, the forecast in both global and regional models are adopted. Among these, the most widely used for global models was the bogusing technique [Lord, 1991], which aim was to reduce the errors in forecast track associated with the weakness and misplacement of hurricanes in the analysis. The bogusing technique consists of inserting an artificial vortex in the global model. The net result of bogusing is a stronger, smaller, more confined and better vortex, which may lead to improved forecast. However, this approach has limitations: it can be successfully applied only to mature, highly symmetric hurricanes and problems related to how to specify a moisture field consistent and vorticity with the imposed vortex are difficult to overcome [Pu and Braun, 2001]. Another more physically-based way to improve the representation of TCs involves additional or localized data as-

simulation, for example satellite derived precipitation or wind (e.g. Hou et al., 2004; Atlas et al., 2005b).

In the last ten years, NASA Goddard has developed a finite-volume General Circulation Model (hereafter fvGCM), which will be discussed in detail. Its dynamical core [described by Lin 2004], thanks to its computational efficiency, has allowed simulations in real time at a resolution of a quarter of degree, which in 2004 was the highest resolution used by any operational GCM in the world [Atlas et al., 2005a]. This is the version used in this study, and is also known as GEOS4. A more recent version named GEOS5 is currently being developed at Goddard.

The high-resolution fvGCM, can produce a realistic TC vortex just with its own dynamics, without the aid of bogusing or of additional data assimilation [Atlas et al., 2005a]. It has produced very good forecast of tropical systems, adequately resolving problems like erratic track, abrupt recurvature, interaction among vortices, reintensification and multiple landfall.

### **2.3 Barotropic instability and tropical cyclogenesis in the fvGCM**

The development of synoptic-scale weather disturbances is often referred to as cyclogenesis, a term that emphasizes the role of relative vorticity in developing synoptic-scale systems. Forecasters have known for some time that tropical cyclones (hereafter TCs) never arise spontaneously, despite all the environmental conditions are considered favorable. Instead, they always

emerge from preexisting circulations of presumably independent dynamical origin [Emanuel, 2003]. No fact of the study of TCs has proven more vexing than understanding and predicting their genesis. TCs depend strongly upon latent and sensible heat fluxes from the ocean [Charney and Eliassen, 1964], since their main source of energy is latent heat release through cumulus convection [Kuo, 1965] and air-sea interaction [Emanuel, 1986; Rotunno and Emanuel, 1986]. They need high values of low-level vorticity, a large scale low-level convergent and upper-level divergent environment and lack of vertical shear. One of the most important components for cyclogenesis is presence of horizontal shear [Reale and Atlas, 2000] and therefore conditions favorable for barotropic instability [McBride and Zehr, 1982]

Track and intensity forecast have been, and are currently being evaluated by the NASA Goddard Laboratory for Atmospheres science team. In this work we will instead investigate the capability of the fvGCM to produce tropical cyclogenesis. Barotropic instability was referred to as a purely theoretical and idealized phenomenon. However, in this study we show that, in spite of the atmosphere being fully baroclinic, a very short-lived and localized form of barotropic instability occurs in the fvGCM during the early cyclogenetic phase. Tropical cyclogenesis is one of the most complex and difficult problems for any model at any resolution, including regional models. In fact, it is very difficult for any model to start a TC circulation just from the initial conditions (hereafter ICs) without some additional information, be it bogus or additional, high resolution, localized data.

In this work, we will analyze a set of ten 5-day fvGCM forecast for the period between August 24 and September 3, 2004. This period was chosen because of the simultaneous appearance of a developing system (Hurricane Frances) and a non-developing system. A description of the fvGCM and a short synoptic discussion of Hurricane Frances is provided. It is then shown that the model has the capability of developing realistic tropical cyclones. The focus is to attempt to understand the mechanism of the early cyclogenetic stage. Therefore, we hypothesize that barotropic instability plays a role in tropical cyclogenesis. To investigate this role, we will analyze the structure of a developing versus non-developing system.

### 3 The Model

The finite-volume General Circulation Model (fvGCM) is an atmospheric global modeling system based on a finite-volume dynamical core, documented by Lin[2004], with terrain-following Lagrangian control volume discretization of the basic conservation laws: mass, momentum and total energy. More than 10 years of effort have been necessary to develop the fvGCM at NASA Goddard Space Flight Center (GSFC). The most fundamental steps of the fvGCM are: 1) development of algorithms for transport processes of water vapor [Lin et al., 1994]; 2) development of multidimensional Flux-Form Semi-Lagrangian Transport scheme (FFSL) [Lin and Rood, 1996]; 3) adaptation of the FFSL algorithm to the shallow water dynamical framework [Lin and Rood, 1997]; 4) development of a simple finite-volume integration method for computing pressure gradient in general terrain following coordinates [Lin, 1997].

An important aspect of the fvGCM development is its high computational efficiency. The fvGCM design was aimed to optimize performance on a variety of computational platforms including distributed memory, shared memory and hybrid architectures. The high resolution fvGCM used for this study was developed as a part of the ALTIX project and was run in 2004 and 2005 as a part of the NASA Project Hurricane on one node of the SGI/Altix system, named Columbia, operational at the NASA GSFC Ames Research Center [Atlas et al, 2005a].

The fvGCM exceptionally high computational efficiency, which allows a 5-day global forecast at a resolution of a quarter of a degree to be completed in about one hour, made ultra-high resolution a reality for global modeling (weather, and climate applications). To resolve tropical weather systems which have a resolution of ten or hundreds of km represents an important step. During 2004, the model was run at a 0.25 degree resolution producing remarkable hurricane forecasts (Atlas et al., 2005). In 2005, experiments were done by further doubling the horizontal resolution to 0.125 degrees, which makes the fvGCM comparable to the first mesoscale resolving General Circulation Model at the Earth Simulator Center (Ohfuchi et al., 2004). The 0.25 degree fvGCM was one of the first very high resolution GCMs running experimentally on twice-daily basis, and provide very good landfall and track predictions of the major hurricanes in 2004 [Shen et al, 2006]. The reason why the resolution was doubled to 0.125 degree was to further investigate the impact of increasing resolution on weather and hurricane prediction.

All the runs analyzed as a part of this project are initialized with global ICs for the dynamic fields provided by the National Centers for Environmental Predictions (NCEP). These are interpolated horizontally and vertically [Lin, 2004], but no additional data assimilation or bogusing of any kind is performed [Atlas et al., 2005a].

## 4 Cyclogenesis in August 2004

This project is focus on a ten-day period in the 2004 hurricane season. This devastating season resulted in twenty-seven federal disaster declarations covering fifteen states, the Virgin Islands and Puerto Rico. The ten-day period was selected because there were two tropical systems simultaneously: a developing (Hurricane Frances) and a non-developing one (tropical wave).

Frances was a Cape-Verde hurricane that reaches an intensity of category 4 hurricane and started as a tropical depression on 0000 UTC 25 August 2004. It strengthened to a tropical storm during 25 August 2004 reaching hurricane strength at 0000 UTC 26 August. Initially Frances moved westward on the south side of the Bermuda-Azores high. Then it turned west-northwestward on 26 August. The hurricane turned westward late on 29 August while it slowly weakened during a concentric eyewall cycle. Re-intensification began on 30 August, and Frances reached a second peak intensity of 125 kt (category 4) late on 31 August as it passed north of the Leeward and Virgin Islands. Frances made landfall in San Salvador Island, Bahamas (1930 UTC 2 September), Cat Island, Bahamas (0530 UTC 3 September), Eleuthera Island, Bahamas (1000 UTC 3 September), Grand Bahama Island, Bahamas (1000 UTC 4 September), Hutchinson Island, Florida (0430 UTC 5 September), Aucilla River, Florida at 1800 UTC 6 September (Beven, 2004).

Frances forms at 00z25Aug2004 becoming eventually a category 4 hurricane. In figure 1 the official observed National Hurricane Center (NHC)

‘best track’ (hereafter BT) or observed track of Frances is shown, together with the fvGCM forecasts initialized 0000 UTC 24, 25, 26, 27, 28, 29 and 30 August.

In the first simulation (initialized on the 24th), Frances is not present in the observations at the time of initialization. However, the model rapidly creates a vortex which at first moves to the west and then recurves to the north, thus correctly predicting the formation and the early track of the system. The runs initialized on the 25th, 26th and 27th have the advantage of starting at a time in which Frances is already present in nature but are affected by another problem. In spite of Frances being present in the observations, its definition in the ICs is very poor (partly due to the relatively low resolution of the NCEP global analysis).

In Fig. 2, observed and forecast sea level pressure (slp) is shown. The forecast refers to the runs initialized at 00z from August 24 to September 3, 2004. The first run initialized on the 24th shows the creation of a vortex without having any information in the ICs. The other runs do have a vortex in the ICs, but at the initialization time, the observed minus analyzed slp difference is of 8 hPa at 00z26Aug, 24 hPa at 00z27Aug, and *46 hPa* at 00z28. In spite of this limitation, the fvGCM tries to build a realistic vortex in about 120 hours. The slp center predicted by the model reaches values comparable to the observed one (particularly in the run initialized on the 30th, 960 hPa), thus compensating the deficient initialization.

The fvGCM is therefore capable of producing two types of cyclogenetic

processes. One is ‘true’ cyclogenesis, in which the model predicts the formation of a cyclone which has not occurred yet in nature but that will form in the near future (such as the run initialized at 00z24Aug04). The other is a cyclogenesis in which the model compensates a deficient and weak vortex in the ICs and rapidly tries to reach the true observed intensity of the TC. This is the case of all subsequent runs where a substantial difference between observed and analyzed center slp is present in the initial conditions. Both processes are possible because the model builds a realistic, dynamically consistent vortex.

In fact, Figure 3, shows the forecast of the vertical cross section of wind magnitude (in  $ms^{-1}$ ), temperature (in  $^{\circ}C$ ) and relative vorticity (in  $s^{-1}$ ) across the storm center for the ICs (00z24Aug), and the 24, 48, 72, 96, 120 hour forecast. The development of a tropical cyclone-like vortex is evident. In the ICs, only a tropical wave can be seen and there is no warm core. However, after 48 hours of integration, (upper right) an eye-like feature (low-speed column and wind maxima on the lower levels on each side of the eye) appears together with a warm core and a rapid increase in low- and mid-level cyclonic vorticity up to the magnitude of  $10^{-4} s^{-1}$ . This increase in relative vorticity is a proof of the capability of the fvGCM to create a realistic and dynamically consistent cyclone. In the subsequent panels (72, 96, and 120 hour forecast) the storm becomes more and more intense, acquiring a very realistic scale (radius of max. wind much less than 50 km). Therefore, the model correctly predicts the formation of a deep vortex after the 25th

(in agreement with the observations) starting without a cyclone in the ICs (00z24Aug). Figures 4 and 5 show the same cross-sections as in Fig. 3, but for the runs initialized on 25 and 31 August. At the initialization times for this run there is already a vortex in the ICs, although weaker than observed. The model however rapidly builds a storm, with ever greater intensity and prominent warm core than the previous runs.

Tropical cyclogenesis is a very complex process arising from several different contributing mechanisms. In this particular work we want to understand which is the triggering mechanism to start a circulation in the model. Therefore we investigate the role that barotropic instability may play in the early stage of tropical development. The verification of Kuo's necessary condition for barotropic instability can be tested since the flow is predominantly zonal. The quantity  $K(y) = 0$  can be conceived as an indicator of where barotropic instability is possible, in response to the shear of the zonal component of the wind. In Figure 6, the quantity  $K(y)$  calculated at 850 hPa is plotted against the sea level pressure and zonal wind for hurricane Frances. It appears that the line  $K(y) = 0$  crosses the storm center at all times. This situation does not change at different levels. In fact, Figure 7, a meridional cross section at the center of the storm, shows that the quantity  $K(y) = 0$  crosses the storm center throughout the entire troposphere. Therefore, the model creates a barotropically unstable column from the surface through the tropopause. These findings are suggestive that barotropic instability is not an abstract theoretical simplification but plays some role in the early tropical

development.

Conversely, Figures 8 and 9, display the same quantities calculated in Figures 6 and 7 but for a non-developing system. The quantity  $K(y) = 0$  does not cross the center of the system in this case. In fact, Figure 9 shows that the model never creates a barotropically unstable column throughout the entire troposphere.

## 5 Summary and Conclusions

In this internship we have provided some evidence that the quarter of a degree resolution NASA fvGCM has the capability to produce tropical cyclogenesis. To understand what can be the triggering mechanism we hypothesize that barotropic instability plays an important role in the early stage of tropical development. To investigate this we calculated the Kuo's necessary condition for barotropic instability  $K(y) = 0$  for a case of a developing system and a case of non-developing system. In particular, the model shown that  $K(y) = 0$  is satisfied only on a vertical column centered on the developing system. Although with a very limited sample these findings suggest that barotropic instability is a crucial mechanism for tropical cyclogenesis and is correctly reproduced in the model. Moreover, we are suggesting that the fvGCM dynamics and the quarter of the degree resolution can have a significant positive impact on the representation of tropical cyclogenesis. In fact, it was shown that the model has some skill in predicting the formation of a cyclone which does not yet exist at the time of the initialization but will form in the subsequent hours. Moreover, the fvGCM also can create a deep tropical cyclone starting from an under-represented vortex in the ICs. In this case the fvGCM compensates a deficient initialization (i.e., an initialization in which the IC vortex is poorly defined and much less deep than the observed one), provided it has a sufficient spin-up time.

Further investigation, possibly to become part of the subject of a Ph.D.

dissertation, would be needed to understand the relationship between tropical cyclogenesis capabilities and model's resolution. In other words, by doing several experiments with same ICs at different, lower or higher resolutions (such as  $0.5^\circ$  ,  $1.0^\circ$ ), or at  $1/8$  degree we would like to investigate if there is a critical resolution which enables the fvGCM to start producing tropical cyclogenetic processes. Other experiments could include a comparison between models having the same resolution and different dynamical cores. In this way we may be able to separate the impact of pure resolution from the impact of the finite-volume dynamical core.

By facing these very high global resolutions several problems may arise. Preliminary experiments done in the Laboratory for Atmospheres at NASA GSFC show that the parametrization schemes may reach their applicability limits at very high resolution, because the model starts explicitly resolving the largest convective systems. Therefore, we would like to explore the behavior of various convective schemes at different resolutions.

The very high resolution made possible by the fvGCM opens a very fascinating new horizon in dynamic meteorology, because for the first time a model can simultaneously resolve global and synoptic scales together with mesoscale. It is possible that to have a mesoscale-resolving global model may shed light on the energetics of processes simultaneously ranging through different scales in a way which has never been done before.

## REFERENCES

- Asnani, G. C., 2005: *Tropical Meteorology.*, Nebula Press, 35-93.
- Atlas, R., O. Reale, B. W. Shen, S. J. Lin, J. D. Chern, W. Putman, T. Lee, K. S. Yeh, M. Bosilovich, and J. Radokovich, 2005a: Hurricane forecasting with the high-resolution NASA finite volume general circulation model. *Geophys. Res. Lett.*, **32**, 2-5.
- Atlas, R., A. Y. Hou, and O. Reale, 2005b: Application of SeaWinds scatterometer and TMI-SSM/I rain rates to hurricane analysis and forecasting. *J. Photogrammetry and Remote Sensing*, **59**, 233-234.
- Beven, J., 2004: Tropical Cyclone Report Hurricane Frances. *Available at <http://www.nhc.noaa.gov/2004frances.shtml>*
- Charney, J. G., and Eliassen, 1964: On the growth of the hurricane depression. *J. Atmos. Sci.*, **21**, 68-75.
- Emanuel, K. A., 1986: An air-sea interaction theory of tropical cyclones. Part I: Steady state maintenance. *J. Atmos. Sci.*, **43**, 585-604.
- Emanuel, K. A., 2003: Tropical Cyclones *Ann. Rev. Earth Planet Sci.*, **31**, 92-94.
- Holton, J. R., 2004: *An introduction to Atmospheric Dynamics.* Elsevier Academic Press, Burlington, 229-309.
- Hou, A. Y., S. Zhang, and O. Reale, 2004: Variational continuous assimilation of TMI and SSM/I rain rates: impact in GOES-3 hurricane analyses and forecast. *Mon. Weather Rev.*, **132 (8)**, 2094-2109.

- Kuo, H. L., 1949: Dynamic instability of two-dimensional non-divergent flow in a barotropic atmosphere. *J. Meteor.*, **6**, 105-122.
- Kuo, H. L., 1965: On the formation and intensification of tropical cyclones through latent heat release by cumulus convection. *J. Atmos. Sci.*, **22**, 48-63.
- Kurihara, Y. M., A. Bender, R. E. Tuleya, and R. Ross, 1990: Prediction experiments of hurricane Gloria (1985) using a multiply nested movable mesh model. *Mon. Weather Rev.*, **118 (10)**, 2185-2198.
- Lin, S. J., 1997: A finite-volume integration method for computing pressure gradient forces in general vertical coordinates. *Q. J. R Meteorol. Soc.*, **123**, 1749-1762.
- Lin, S. J., and R. B. Rood, 1996: Multidimensional flux-from semi-Lagrangian transport schemes. *Mon. Weather Rev.*, **124**, 2046-2070
- Lin, S. J., and R. B. Rood, 1997: An explicit flux-from semi-Lagrangian transport schemes. *Mon. Weather Rev.*, **124**, 2477-2498
- Lin, S. J., W. C. Chao, Y. C. Sud, and G. Q. Walker, 1994: A
- Lin, S. J., W. C. Chao, Y. C. Sud, and G. Q. Walker, 1994: A class of the van Leer-type transport schemes and its applications to the moisture transport in a general circulation model. *Mon. Weather Rev.*, **122**, 1575-1593
- Lord, S. J., 1991: A bogusing system for vortex circulations in the National meteorological Center global forecast model. *Pre-prints, 19th*

- Conference on Hurricanes and Tropical Meteorology, Miami, FL, Am. Meteorol. Soc.*, **12**, 328-330.
- McBride, J., and R. Zehr, 1981: Observational analysis of tropical cyclone formation. Part II: Comparison of non-developing versus developing systems. *J. Atmos. Sci.*, **38**, 1132-1154.
- Ooyama, K., 1964: A dynamical model for the study of tropical cyclone development. *Geofisi. Int.*, **4**, 187-198.
- Pu, Z. H., S. Brau, 2001: Evaluation of bogus vortex techniques with four-dimensional variational data assimilation. *Mon. Weather Rev.*, **129**, 2023-2039.
- Reale, O., and R. Atlas., 2000: Tropical cyclone-like vortices in the extratropics: observational evidence and synoptic analysis. *Weather and Forecasting.*, **16**, 7-26.
- Rotunno, R., and K. Emanuel, 1987: An air-sea interaction theory of tropical cyclones. Part II: Evolutionary study using a nonhydrostatic axisymmetric numerical model. *J. Atmos. Sci.*, **44**, 542-561.
- Shen, B. W., R. Atlas, J. D. Chern, O. Reale, S. J. Lin, T. Lee, and J. Chang, 2006a: The 0.125 degree finite-volume general circulation model on the NASA Columbia supercomputer: Preliminary simulations of mesoscale vortices. *Geophys. Res. Lett.*, **33**, 1-2.
- Shen, B. W., R. Atlas, O. Reale, S. J. Lin, J. D. Chern, J. Chang, C. Henze, and J. L. Li, 2006b: Hurricane forecast with a global

mesoscale-resolving model: Preliminary results with Hurricane Katrina. *Geophys. Res. Lett.*, **33**, 1-5.

## List of Figures

1	fvGCM simulations for Hurricane Frances compared with the observed track by the National Hurricane Center (NHC). Each dot represents the center position at 6-hour time increments . . . . .	25
2	fvGCM predicted center pressure for Hurricane Frances compared to the NHC observations. . . . .	26
3	Vertical cross section relative to the ICs (upper left) INIT 00z24Aug04. The other panels refer to 24,48,72,96,120 hFCs. Plotted are wind speed ( $\text{ms}^{-1}$ , shaded), temperature ( $^{\circ}\text{C}$ , solid black line), relative vorticity ( $\text{s}^{-1}$ ), red and blue lines. . . . .	27
4	Same as figure three but initialized at 00z25Aug04. Top left are the ICs. . . . .	28
5	Same as figure three but initialized at 00z31Aug04. Top left are the ICs. . . . .	29
6	Sea level pressure (hPa) and values of the function $K(y) = \frac{\partial}{\partial y}[f(y) - \frac{\partial U}{\partial y}]$ ( $\text{m}^{-1} \text{s}^{-1}$ ), calculated at 850 hPa, at (a) 12z25Aug04, (b) 18z26Aug04, (c) 18z30Aug04, and (d) 00z02Sep04 for runs initialized respectively at 00z 24,25,27,31 Aug. Contours at $8 \times 10^{-10} \text{ m}^{-1} \text{ s}^{-1}$ . Red and blue shading represent the zonal wind ( $\text{ms}^{-1}$ ). . . . .	30

- 7 Vertical cross section of the function  $K(y) = \frac{\partial}{\partial y}[f(y) - \frac{\partial U}{\partial y}]$  ( $\text{m}^{-1} \text{s}^{-1}$ ) and zonal wind, calculated at 850 hPa, at (a) 12z25Aug04, (b) 18z26Aug04, (c) 18z30Aug04, and (d) 00z02Sep04 for the runs initialized respect at 00z 24,25,27,31 Aug. Contours at  $8 \times 10^{-10} \text{ m}^{-1} \text{ s}^{-1}$ . Red and blue shading represents the zonal wind ( $\text{ms}^{-1}$ ). . . . . 31
- 8 Same as Figure 6 but for a non-developing system, at (a) 00z24Aug04, (b) 00z25Aug04, (c) 12z25Aug04, and (d) 00z25Sep04. 32
- 9 Same as Figure 7 but for a non-developing system, at (a) 00z24Aug04, (b) 00z25Aug04, (c) 12z25Aug04, and (d) 00z25Sep04.

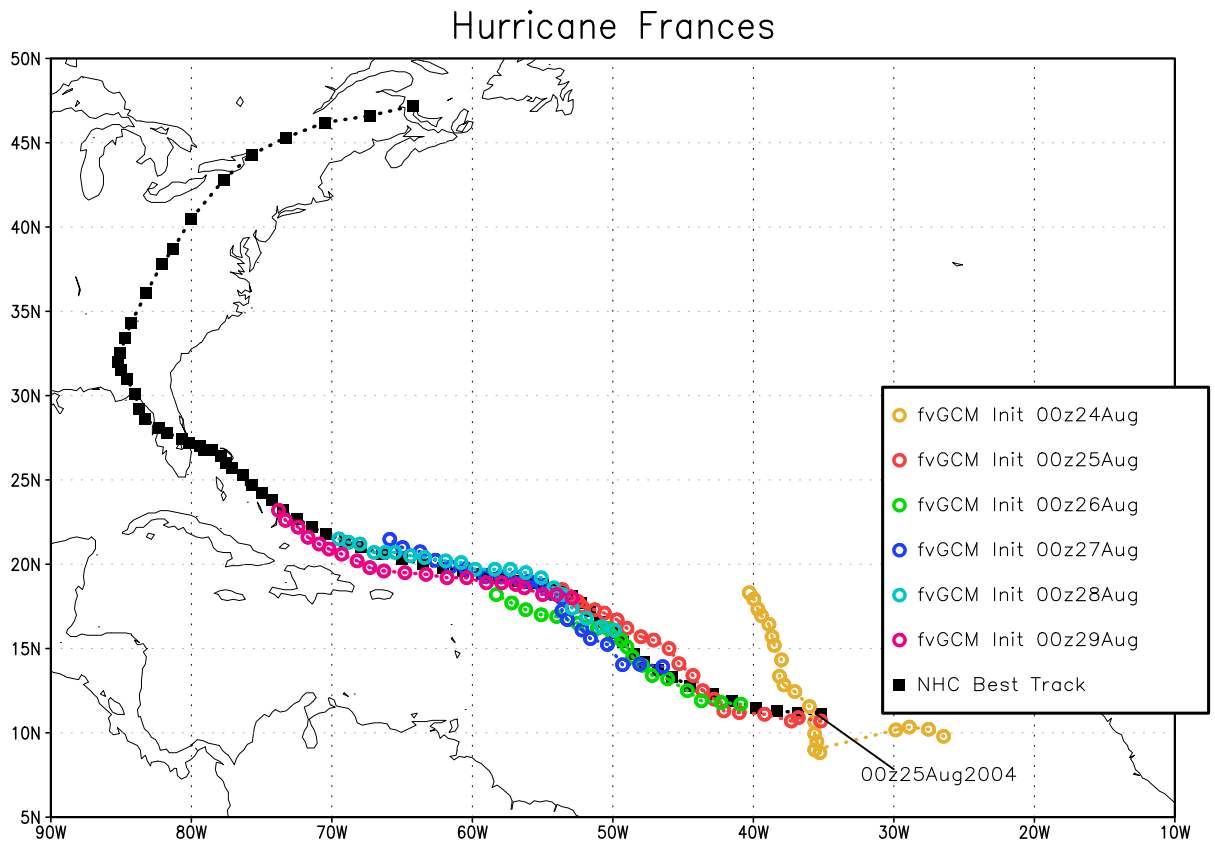


Figure 1: fvGCM simulations for Hurricane Frances compared with the observed track by the National Hurricane Center (NHC). Each dot represents the center position at 6-hour time increments

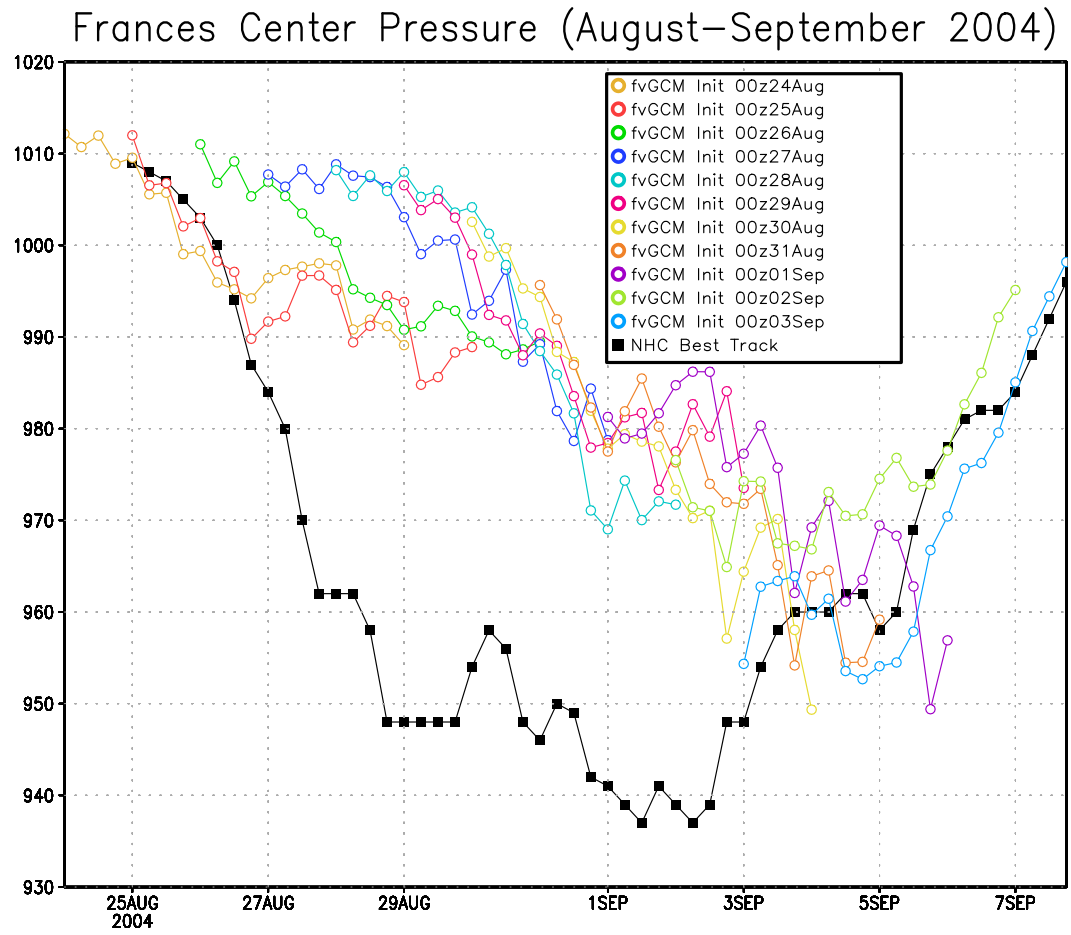


Figure 2: fvGCM predicted center pressure for Hurricane Frances compared to the NHC observations.

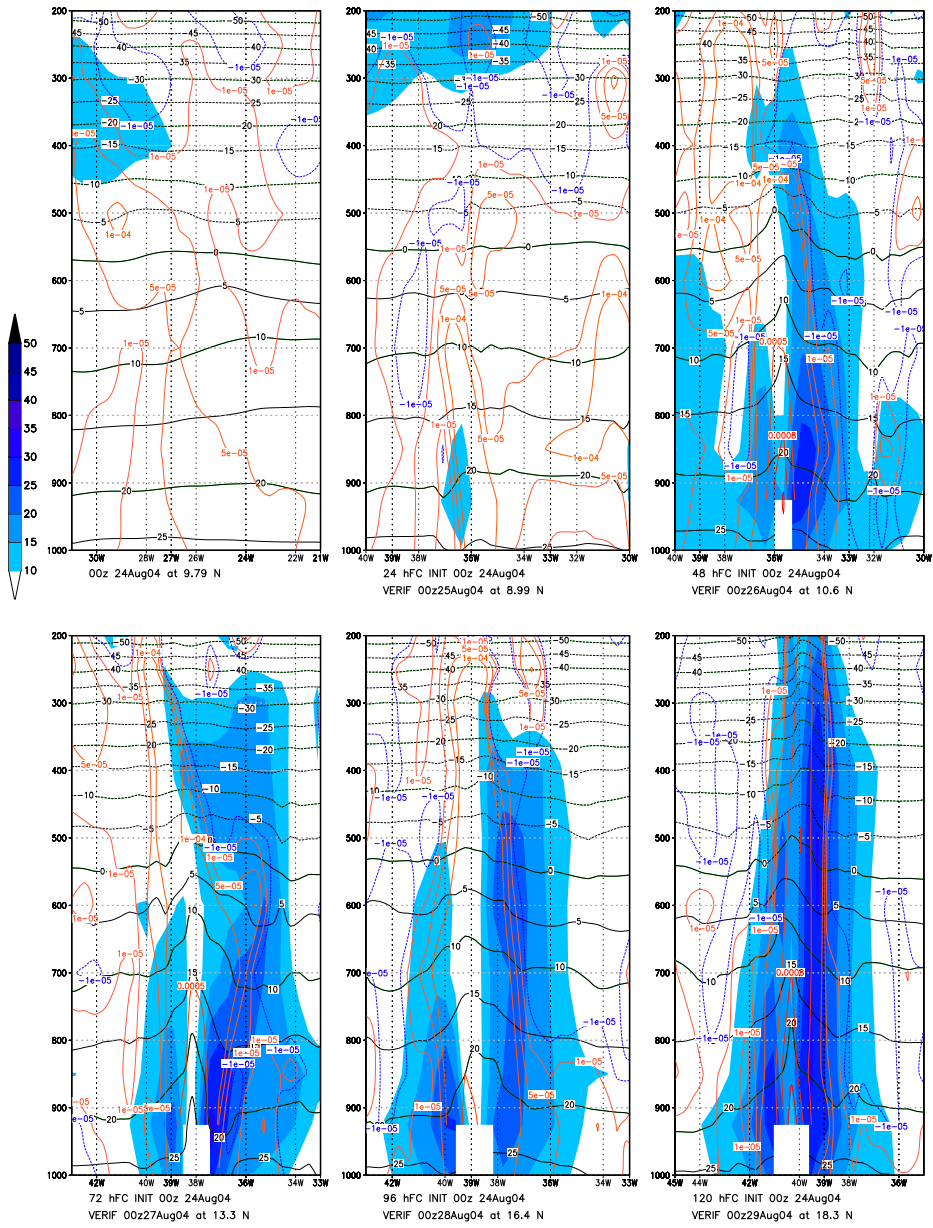


Figure 3: Vertical cross section relative to the ICs (upper left) INIT 00z24Aug04. The other panels refer to 24,48,72,96,120 hFCs. Plotted are wind speed ( $\text{ms}^{-1}$ , shaded), temperature ( $^{\circ}\text{C}$ , solid black line), relative vorticity ( $\text{s}^{-1}$ , red and blue lines).

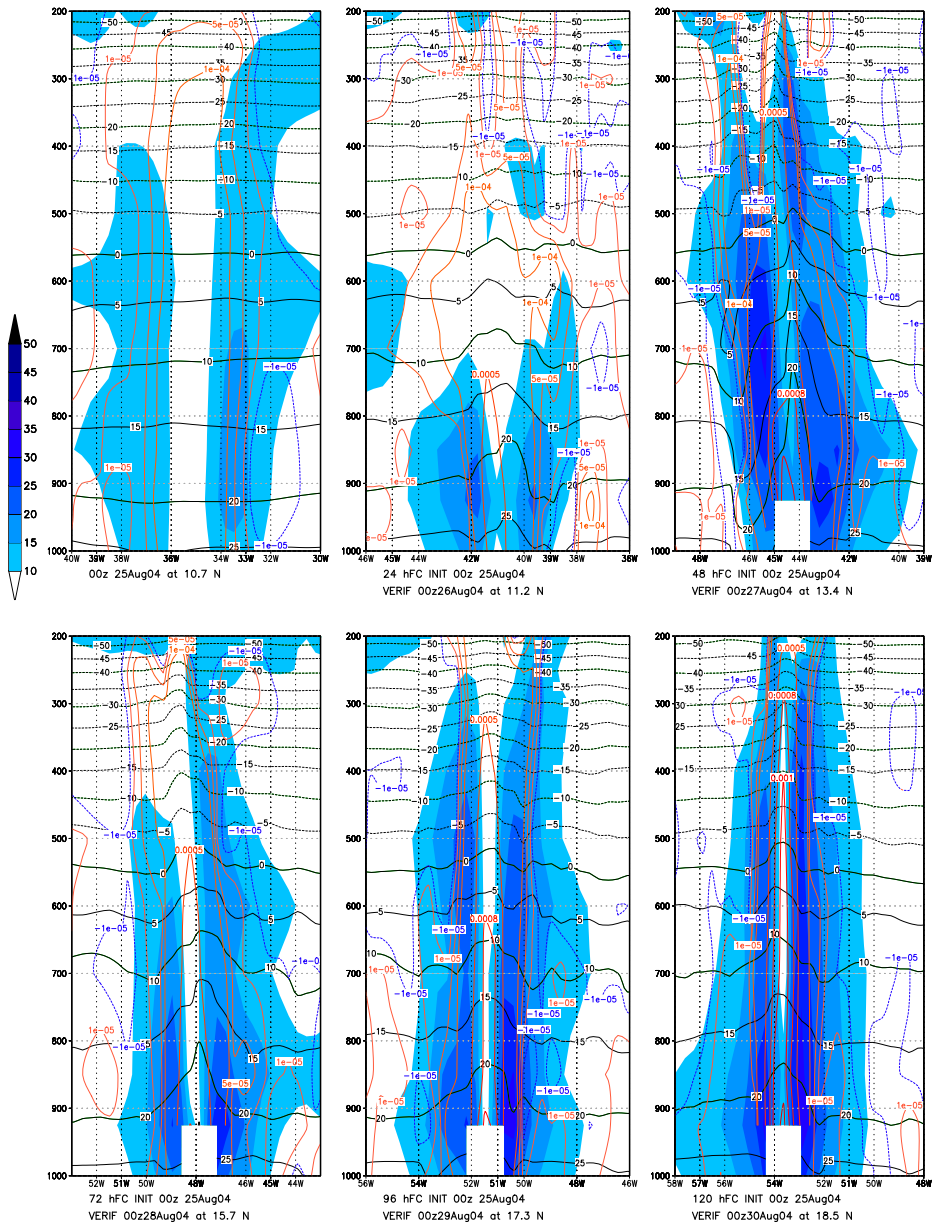


Figure 4: Same as figure three but initialized at 00z25Aug04. Top left are the ICs.

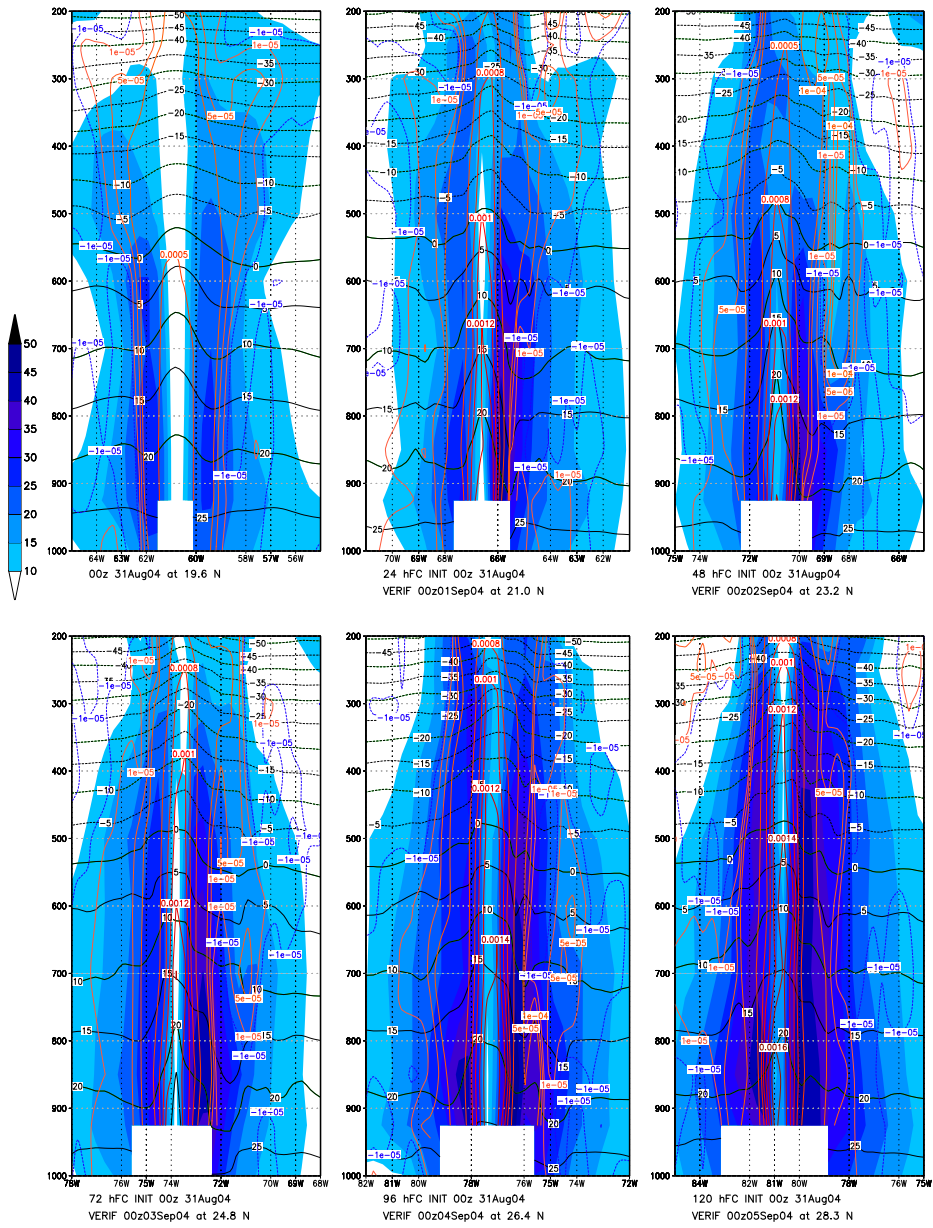


Figure 5: Same as figure three but initialized at 00z31Aug04. Top left are the ICs.

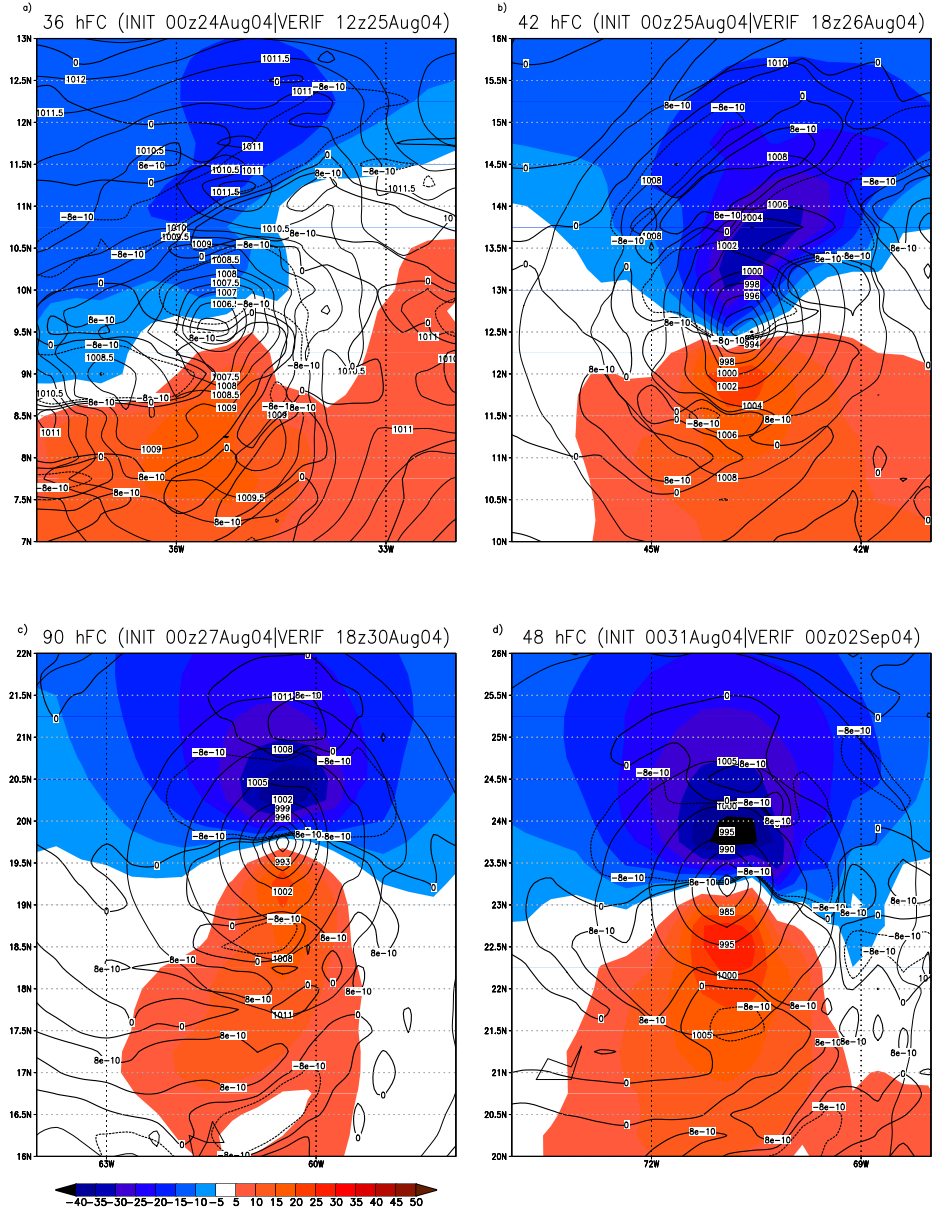


Figure 6: Sea level pressure (hPa) and values of the function  $K(y) = \frac{\partial}{\partial y}[f(y) - \frac{\partial U}{\partial y}]$  (m<sup>-1</sup> s<sup>-1</sup>), calculated at 850 hPa, at (a) 12z25Aug04, (b) 18z26Aug04, (c) 18z30Aug04, and (d) 00z02Sep04 for runs initialized respectively at 00z 24,25,27,31 Aug. Contours at  $8 \times 10^{-10}$  m<sup>-1</sup> s<sup>-1</sup>. Red and blue shading represent the zonal wind (ms<sup>-1</sup>).

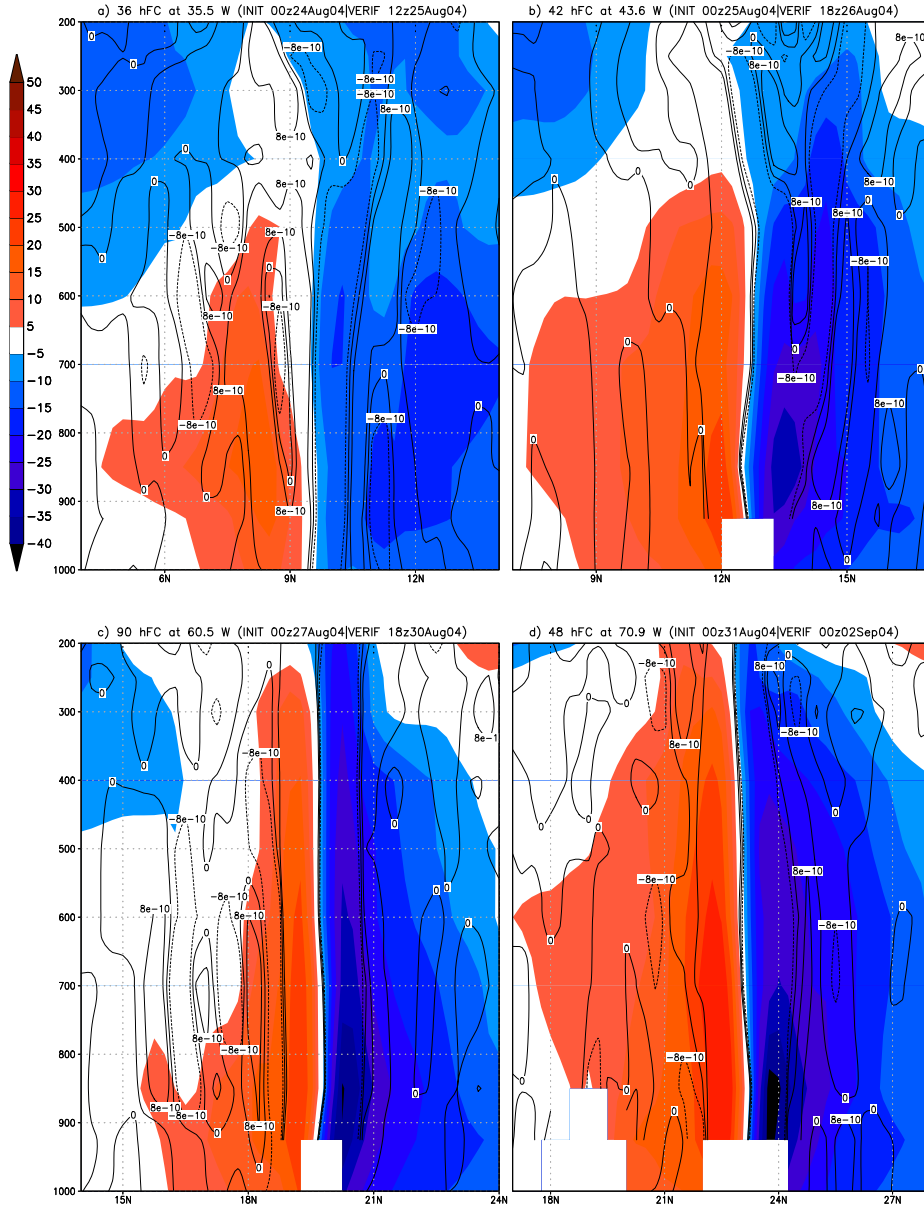
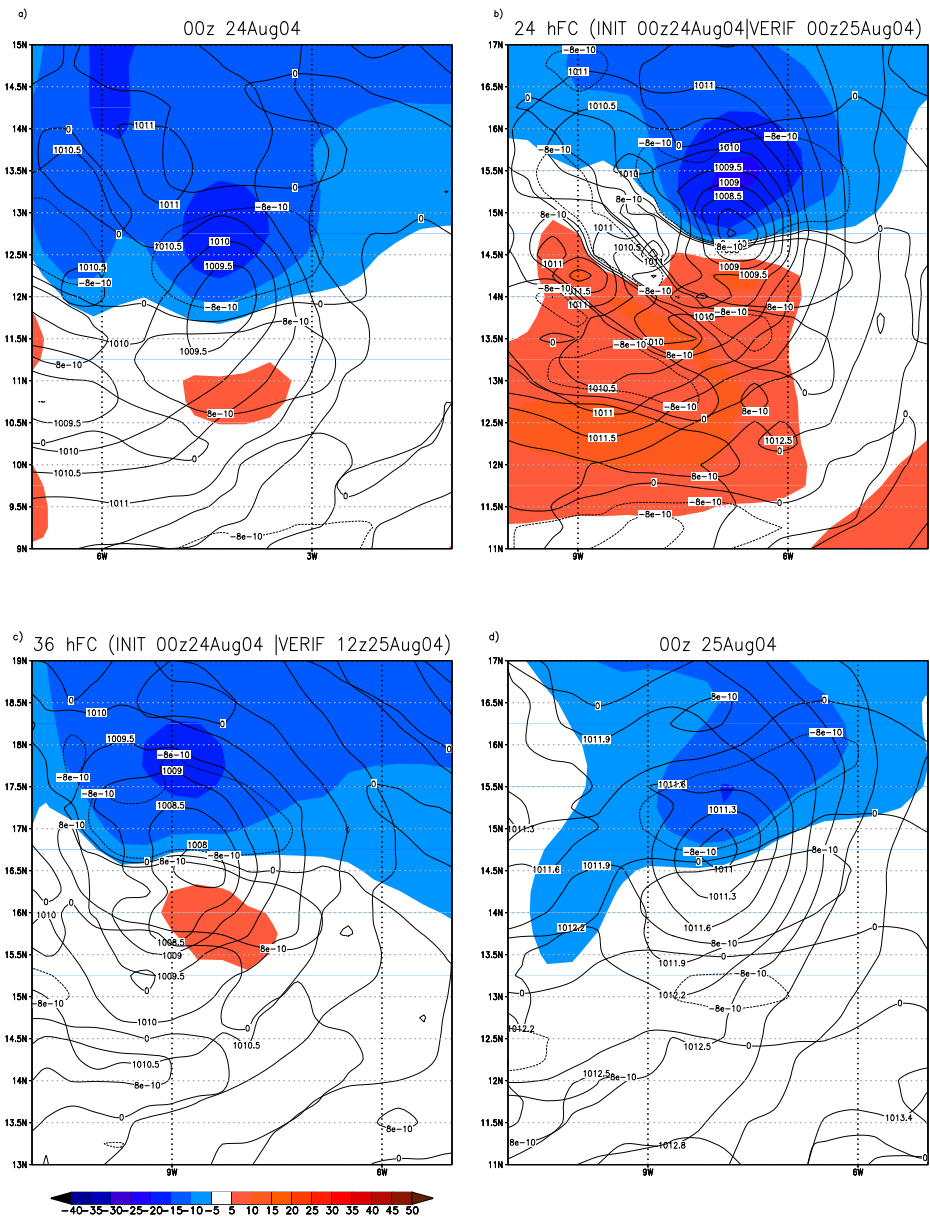


Figure 7: Vertical cross section of the function  $K(y) = \frac{\partial}{\partial y}[f(y) - \frac{\partial U}{\partial y}]$  ( $\text{m}^{-1} \text{s}^{-1}$ ) and zonal wind, calculated at 850 hPa, at (a) 12z25Aug04, (b) 18z26Aug04, (c) 18z30Aug04, and (d) 00z02Sep04 for the runs initialized respect at 00z 24,25,27,31 Aug. Contours at  $8 \times 10^{-10} \text{ m}^{-1} \text{ s}^{-1}$ . Red and blue shading represents the zonal wind ( $\text{ms}^{-1}$ ).



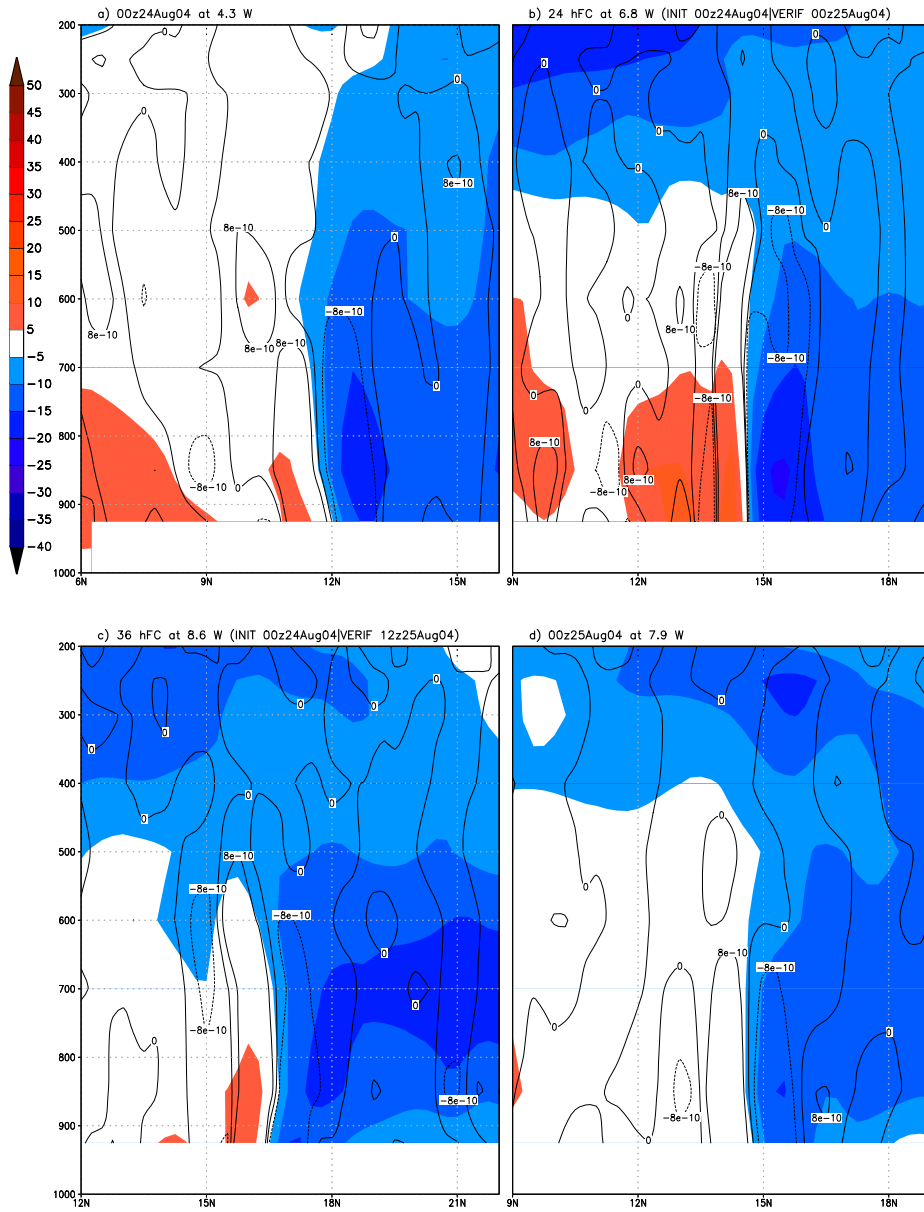


Figure 9: Same as Figure 7 but for a non-developing system, at (a) 00z24Aug04, (b) 00z25Aug04, (c) 12z25Aug04, and (d) 00z25Sep04.